Chinese Journal of Analytical Chemistry 50.7 (2022) 100107

Contents lists available at ScienceDirect

Chinese Journal of Analytical Chemistry

journal homepage: www.elsevier.com/locate/cjac

A novel SERS-based rapid and sensitive assay for methidathion detection in various fruits

Xi-Xi HUANG[1], Yuan-Chao FAN[1], Shi-Liang CHEN*, Xiao-Jing CHEN, Shujat ALI, Xi CHEN, Lei-Ming YUAN, Wen SHI, Cheng-Xi JIANG, Guang-Zao HUANG*

College of Electrical and Electronic Engineering, Wenzhou University, Wenzhou 325035, China

ARTICLE INFO

Key words:
Methidathion
Organophosphorus pesticides (OPs)
Rapid detection
Fruits
Surface enhanced Raman scatting (SERS)
Multivariate analysis (MVA)

ABSTRACT

This study establishes a sensitive and facile method for trace detection of methidathion (MTDT) by using spherical Ag nanoparticles (Ag NPs) based on surface enhanced Raman scatting (SERS). During detection, MTDT was rapidly alkaline hydrolyzed through S_N2 substitution reaction and generated a thiadiazolin derivative with a more stronger Raman activity. After removing hydroxide ions from the solution, a limit of detection (LOD) as low as 0.33 ppb was achieved, which is two orders of magnitude below as compared to the non-hydrolysis group. Base on a self-developed and fast (10 min) pre-treatment method, MTDT was successfully detected in six kinds of fruit. The detection limits were ranged from 5–15 ppb, which were much lower than the maximum residue limit (MRL) required by China, US and the EU. Moreover, multivariate analysis (MVA) method was used for quantitative analysis in apple spiked samples, compared with univariate analysis (UVA), a higher determination coefficient (R^2=0.9331) and a better dynamic range (10 ppb–5 ppm) were obtained. The major aim of this work is to provide an operational, fast and sensitive method to specifically detect the MTDT pesticide in real agricultural samples.

1. Introduction

Methidathion (MTDT) is one of the most widely used organophosphorus pesticides (OPs) for the prevention and control of insects in agricultural crops. However, its residue in agricultural products and water is a serious threat due to the high toxicity [1–4]. Therefore, the analysis of MTDT has always been an important research topic in the fields of agriculture, food safety, medicine and environment [4–9].

Previously, various sophisticated and sensitive analytical methods have been used for the detection of MTDT. These methods are based on gas chromatography (GC) [9,10] and GC coupled with mass spectrometry (GC-MS) [11,12], high performance liquid chromatography (HPLC) [13,14] and HPLC coupled with mass spectrometry (LC-MS) [15,16]. However, these methods have the disadvantages of complex sample preparation, time-consuming, expensive equipment, and need professional operators. So, the rapid and facile detection MTDT is still need to be explored further. Alternatively, spectroscopic methods have always been considered as promising detection tool. Fluorescence sensors seem to have relatively high sensitivity but has the drawbacks that cannot specifically identify the target OP molecule and require a long reaction time [17,18]. Surface enhanced Raman scatting (SERS), as a rapid detection technology which can provide an ultra-sensitive “fingerprint” Raman information [19–22], and even overcome the single molecule detection [23,24]. However, there is no great progress in the detection of MTDT [25–27], due to the low Raman response of MTDT molecule. The detection limit has been reported around the ppm level, which is a big gap compared with other technologies. Therefore, it is an urgent need and huge challenge to improve the detection performance of the SERS method for the rapid and sensitive detection of MTDT.

In this work, we developed an incredibly simple and easy method for trace detection of MTDT by only using spherical Ag nanoparticles (Ag NPs) as SERS substrate. The basic strategy is that pure MTDT was rapidly hydrolysed in an alkaline condition via S_N2 substitution reaction and detected in a neutral ionic environment, which led to a signal improvement of more than two orders of magnitude. Consequently, limit of detection (LOD) of 0.33 ppb was achieved. GC-MS and density functional theory (DFT) simulation verified that the increased signal was derived from one of the hydrolysates ((5-methoxy-2-oxo-1,3,4-thiadiazol-3(2*H*)-yl) methanethiolate), which has higher Raman activity and water solubility compared with pure MTDT. Moreover, this detection strategy has been applied in the detection of six kinds of fruit combine with a self-developed pre-treatment method. This pre-treatment method just

* Corresponding authors.
E-mail addresses: Chenshiliang20@163.com (S.-L. CHEN), hguangzao@163.com (G.-Z. HUANG).
[1] Xixi Huang and Yuanchao Fan contributed equally to this work

https://doi.org/10.1016/j.cjac.2022.100107
Received 27 December 2021; Received in revised form 17 March 2022; Accepted 21 April 2022
Available online 25 April 2022
1872-2040/© 2022 Changchun Institute of Applied Chemistry, CAS. Published by Elsevier Ltd. All rights reserved.

includes three simple steps based on the liquid-liquid extraction (LLE) strategy and the whole operation processes can be completed in 10 min. The resulting LODs were ranged from 5–15 ppb in different fruits, which were much lower than the MRL required by China, US and the EU. Furthermore, multivariate analysis (MVA) was adopted to improve the feasibility of quantitative analysis, solved the problem of characteristic variable change and improved the accuracy and stability of the quantitative model compared with univariate analysis (UVA).

This study was dedicated to develop a simple, rapid and sensitive method for the detection of MTDT in fruits and solve the problems of sensitivity and operability in practical application. We believe that the detection method, mechanism and algorithm have great application potential and can be extend to more applications such as food safety, environmental monitoring and clinical diagnosis.

2. Experimental Methods

2.1. Materials and chemicals

Methidathion (99.8%) was purchased from Sinopharm Chemical Reagent Co., Ltd. (Beijing, China). Silver nitrate ($AgNO_3$) was bought from ANPEL Laboratory Technologies (Shanghai) Inc. Trisodium citrate, hydrochloric acid, sodium chloride, ammonium chloride, acetonitrile, petroleum ether (PE), sodium sulfate, sodium hydroxide and ethyl alcohol (EtOH) were purchased from Macklin Biochemical Technology Co., Ltd. (Shanghai, China). Dimethyl thiophosphate (DMTP) was purchased from Beijing VsciChem Technology Co., Ltd (Beijing, China).

2.2. Instrumentation

Transmission electron microscope (TEM, JEM-2100F, Shimadzu Co., Japan) and selected area electron diffraction (SAED) were used to characterize the morphology of Ag NPs. Ultraviolet and visible spectrophotometer (UV-vis 2450, Shimadzu Co., Japan) was used to obtain the UV-visible absorbance spectra. Gas chromatography-mass spectrometry (GC-MS) (7890A, Agilent Technologies, US) was used to identify the components of MTDT alkaline hydrolysates. A portable Raman spectrometer (ATR3110, Optosky Co., Xiamen) was used to adopt the surface plasma resonance scattering signals.

2.3. Preparation of spherical Ag NPs

The Ag NPs were prepared by the sodium citrate reduction method. Briefly, 1 mL of trisodium citrate solution (0.5% wt) was quickly added to 49 mL of $AgNO_3$ aqueous solution (0.01 M) in boiling condition and stirred for 25 min. Then, 0.35 mL of trisodium citrate (1% wt) was added and continuously stirred for 15 min. The resultant reaction mixture was cooled to room temperature, and obtained an earthy-yellow Ag colloid.

2.4. Methods for pre-treatment of fruits and detection

For the pre-treatment, 1 g of fruit homogeneous sample was taken in a 10 mL centrifuge tube, added 4 mL of 7.5% EtOH solution. The sample was ultrasonically extracted for 2 min, and then added 2 g of NaCl solid and continuously extracted (ultrasonically) for 1 min. Then, 2 mL of the supernatant was taken in a 5 mL centrifuge tube and added an equal volume of petroleum ether (PE). After oscillation and stratification, 1 mL of supernatant was taken in another centrifuge tube, and 1 mL of 0.2 M NaOH (in 40% EtOH solution) was added. After vigorous oscillation and stratification, the aqueous phase was taken for testing. During the stratification process, a slight centrifugation (for example, 6000 r min^{-1}, 30 s) was performed to avoid serious emulsification.

For fruit sample detection, 100 μL of the above mixture was mixed with 100 μL of 0.2 M HCl solution. Then, 50 μL of Ag NPs colloid was added, mixed and detected under 785 nm Raman spectrometer.

For standard sample analysis, 25 μL of 1 M sodium hydroxide was added to 200 μL standard sample, and then 25 μL of 1 M HCl was added. Then, 50 μL of Ag NPs colloid were added, mixed and incubated for 2 min, and detected by a 785 nm Raman spectrometer.

2.5. DFT calculations

The optimize structures of hydrolysate molecule (5-methoxy-2-oxo-1,3,4-thiadiazol-3(2*H*)-yl methanethiolate (MTMT)) were analysed by employing the PCM solvent model through Gaussian 09 program based on the B3LYP functional [28,29] and 6-31+G(d) basis sets. The VEDA4 [30] program was used to perform normal-mode analysis. Then, the molecular orbit and simulation Raman spectrum of MTMT were calculated.

2.6. Algorithms for quantitative analysis

Univariate and multivariate analysis methods were used for quantitative analysis. According to the relationship between unitary SERS characteristic peak intensity and MTDT concentrations added in fruit samples, a univariate linear regression (ULR) model was established as the following equation:

$$Y = \beta X + \varepsilon. \tag{1}$$

Y is the predicted value of the sample, representing the dependent variable in the regression model. X is the characteristic value of the sample, representing the independent variable in the regression model. β is the coefficient matrix. and ε is the error term in the regression model.

In multivariate modelling method, the relationship between the intensity of multiple SERS characteristic peaks and MTDT concentrations added in fruit samples was comprehensively considered, and a multivariate linear regression (MLR) model was established as the following equation:

$$Y_{m\times k} = X_{m\times n}\beta_{n\times k} + \in_{m\times k}. \tag{2}$$

$X_{m\times n}$ represents a matrix of m samples and n peak variables, $Y_{m\times k}$ represents a matrix of m samples and k concentration variables. $\beta_{n\times k}$ is the coefficient matrix and $\in_{m\times k}$ is the random error term.

3. Results and discussion

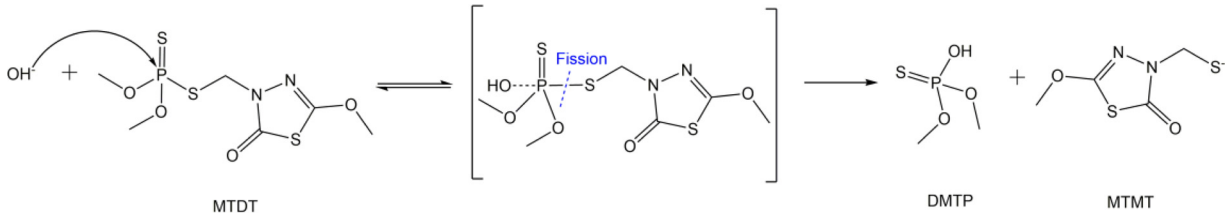
3.1. Characterization of Ag NPs

In this study, Ag NPs were prepared by a sodium citrate reduction method without surfactants. As shown in Fig. 1a, the morphology of Ag NPs appeared spherical with an average size of about 65 nm. Fig. 1b shows the UV-vis spectra of Ag NPs and presents surface plasmon resonance (SPR) peak at 419 nm. SAED pattern in Fig. 1c clearly illustrates four sets of diffraction rings of Ag NPs which assigned to the (111), (200), (220) and (311) planes, and the typical lattices spacing in HR-TEM image (Fig. 1d) further verified the crystal nature [31–35], indicating the Ag NPs were in good agreement with the face-centered-cubic structure [36,37].

Malachite green was used to investigate the enhancement performance of Ag NPs, the SERS and normal Raman spectra of malachite green are shown in Fig. S1. According to the enhancement factor (EF) calculation formula [38,39]:

$$\mathrm{EF} = \frac{N_{\mathrm{bulk}} I_{\mathrm{surf}}}{N_{\mathrm{surf}} I_{\mathrm{bulk}}}, \tag{3}$$

where I_{bulk} and N_{bulk} represent the signal intensity and the number of measured molecules in normal Raman experiment, respectively. I_{surf} and N_{surf} represent the SERS signal intensity and the number of measured molecules on nano-surface of Ag NPs within excited area, respectively. Finally, the EF was calculated to be around 0.92×10^8. The detailed calculation process of EF is available in the supplement information.



Scheme 1. The alkaline hydrolysis pathway of methidathion, following the S_N2 substitution reaction and products the DMTP and MTMT.

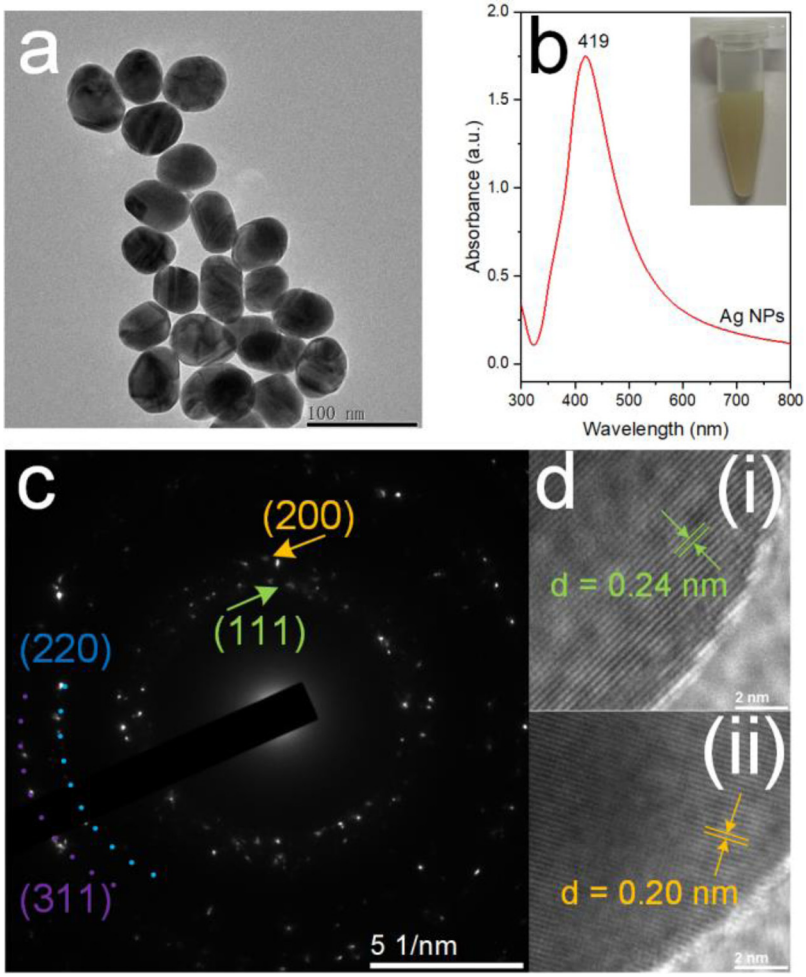


Figure 1. (a) TEM image of Ag NPs. (b) UV-vis spectrum and photograph (inset) of Ag NPs. SAED pattern (c) and HRTEM image (d) of Ag NPs.

3.2. Mechanism and optimization condition of detection method

In this study, the detection method was based on the following two steps. Firstly, the MTDT hydrolysates were obtained by alkaline hydrolysis. Secondly, the coupling effect between Ag NPs was adjusted by hydrochloric acid to obtain the SERS signal of hydrolysates for the indirect detection of MTDT.

For the first step, NaOH was used as the nucleophilic reagent for MTDT alkaline hydrolysis through S_N2 substitution reaction [36,40-43], the reaction pathway is shown in Scheme 1. The hydroxide ions attack on the central P atom, causing the P–S bond to break and generate the $DMTP^-$ and $MTMT^-$. GC-MS results verified the above reaction (Fig. 2a). After the alkaline hydrolysis, the parent ion fragments of DMTP (141 *m/z*) and MTMT (177 *m/z*) appeared at 9.6 and 4.2 min (Fig. S2), respectively.

For the second step, hydrochloric acid was added to the alkaline solution to regulate the acidity and aggregate conditions. Fig. 2b indicates that this step greatly improves the SERS signal of alkaline hydrolysates. Moreover, when the adding acid just neutralized the NaOH (i.e., NaOH (aq) + HCl (aq) → H_2O (l) + NaCl (aq)), the alkaline hydrolysates exhibited the highest signal (Fig. 2c, d). This is equivalent to the NaCl as the aggregator for Ag NPs to realize the coupling effect. Hence, the NaOH concentration during alkaline hydrolysis process directly determines the overall ion components and concentrations in the second step. Fig. S3 shows the impact of NaOH concentration on the SERS signal of hydrolysates under HCl neutralization, and 0.1 M NaOH was selected as the optimal condition in hydrolysis solution. This is because of a higher concentration might cause the excessive aggregation of NPs and scattering signal degradation, a lower concentration might result in inadequate hydrolysis, due to the reaction rate of above second-order (or pseudo first-order) reaction is mainly affected by the concentration of nucleophile. It is well known that the aggregation of NPs is affected not only by the salt concentration but also the interaction time. For obtaining the sensitivity and reproducibility signal, the time-dependent Raman

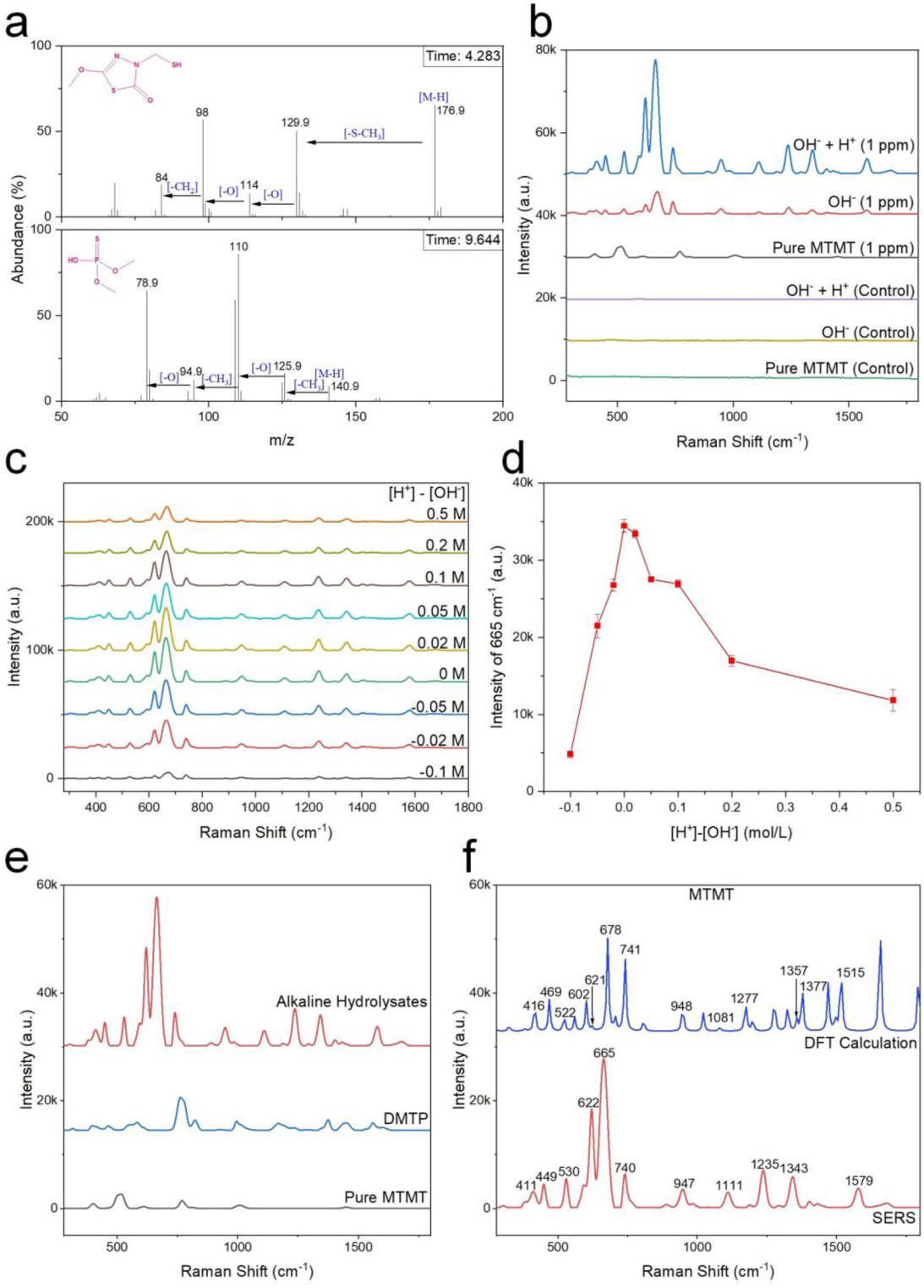


Figure 2. (a) GC-MS results of MTDT hydrolysates. (b) SERS spectra of MTDT (0.1 ppm) obtained from different analytical methods (neutralized after alkaline hydrolysis, only alkaline hydrolysis and non-hydrolysis) by Ag NPs. (c) The impact of acidity on the SERS signal of hydrolysates, and the alkaline hydrolysates exhibited the highest strength at neutralization point, according to the strength curve (d). (e) SERS signals of alkaline hydrolysates, DMTP and pure MTDT. (f) Raman vibrational spectra of MTMT calculated by DFT and SERS spectra of alkaline hydrolysates.

analysis method was used to record the evolution of SERS signals with aggregate time (0–5 min) in different concentrations (0.05, 0.1 and 0.5 ppm) of analyte, Fig. S4a shows that the stability period of SERS signal appeared in the interval of 2 to 3 min for each concentration. Considering the stability, rapidity and sensitivity of detection performance, the optimal signal was selected when the acting time was 2 min. Further-

Table 1
The SERS experimental observed frequencies of skeletal vibration for MTDT alkaline hydrolysates and B3LYP/6-31+G(d) calculated frequencies of MTMT.

SERS(cm^{-1})	DFT calculation(cm^{-1})	Mode descriptions
411	416	N–N–C out-of-plane bending vibration C–S–C stretching and bending vibration
449	469	C–S–C asymmetric stretching vibration
530	522	C–S—C shear vibration
593	602	N=C–S out-of-plane bending vibration and C–N(S) stretching vibration
622	621	N-C–S out-of-plane bending vibration
665	678	C–S(H) stretching vibration
740	741	N–N–C(O) shear vibration C–S(H) stretching vibration
947	948	N–N–C(O) symmetric stretching vibration N–C(S) stretching vibration
1111	1081	C(3H)–O stretching vibration
1235	1277	C-N(S) stretching vibration C–O stretching vibration
1343	13571377	C(O)–N stretching vibration C–H symmetric/asymmetric oscillation of $–CH_2$
1579	1515	C–H oscillation of $–CH_3$

more, signals recorded at 2 min in multiple parallel experiments (Fig. S4b–e) all showed stable results, which further verified the reproducibility of detection.

To better clarify the attribution of SERS signal, Fig. 2e compares the SERS signals of alkaline hydrolysates, DMTP and pure MTDT. It can be seen that the alkaline hydrolysates have the apparent Raman strength advantage, and the DMTP and pure MTDT contributed negligible to the SERS signal of alkaline hydrolysates. Namely, the distinctive SERS signal of MTDT alkaline hydrolysates was mainly presented by MTMT. This was attributed to the bonding effect between the sulfhydryl group and silver, which not only ensured the competitive advantage of the hydrolysate on the nano-surface, but also provided the prerequisite for further charge transfer (CT) between the adsorbate and metal [44]. In parallel, we used DFT method to calculate the Raman vibrational spectra of MTMT and found that it was in good consistent with the SERS spectra of alkaline hydrolysates, especially in the range of low wavenumber (Fig. 2f). The vibration attribution of corresponding characteristic peaks is represented in Table 1. Obviously, the C–S stretch vibration has the most Raman activity and shows the highest SERS peak at 662 cm^{-1}. This indicated that the strategy of alkaline hydrolysis of MTDT which led to the exposure of the C–S group made a great contribution to the Raman signal. It was also worth noting that, the Raman activity of heterocyclic deformation vibration (out-of-plane) was not prominent in the simulated spectra (at 621 cm^{-1}), whereas the opposite was obvious in SERS result (at 622 cm^{-1}). This may be caused by the CT between silver and binding molecule. Because of the LUMO + 1 orbit mainly located in the heterocycle group (Fig. S5), when the CT excitation was shifted from the HOMO of silver to the LUMO + 1 of MTMT, it significantly promoted the chemical enhancement which led to an increasement of amplitude in the corresponding heterocyclic vibration mode [44–46]. Other distinctive characteristic peaks, such as at 530, 740, 1235 and 1343 cm^{-1}, were also observed. These peaks provided reliable characteristic variables for the multivariate quantitative analysis.

To the best of our knowledge, there is no other organophosphorus pesticide molecules that can produce MTMT via S_N2 substitution reaction in alkaline condition, so the above-mentioned method can be used as a specific detection method for MTDT. Hypothetically, if there are other molecules that can generate the same leaving group, it might be a better idea to categorize them together.

3.3. The detection limit of MTDT standard sample

Based on the above optimization approach, the SERS spectra of MTDT under different concentration gradients were achieved (Fig. 3a). The highest peak, 662 cm^{-1}, was used as the characteristic peak for MTDT sensitive identification. Then, the three times of signal noise ratio (SNR) was considered as the threshold of detection limit, and 0.33 ppb was determined as the LOD. This value is more than two orders of magnitude below the non-hydrolysis group (i.e., 50 ppb, Fig. S6). Moreover, the method showed a good linear relationship in the range of 0.33 ppb to 1 ppm (Fig. 3b).

3.4. Pre-treatment method for fruits

The pre-treatment in various fruits adopt the strategy of LLE, which is divided into the following three steps. Firstly, the fruit was homogenized and ultrasonically extracted with 7.5% ethanol. Secondly, the obtained supernatant was extracted with petroleum ether (PE). Thirdly, the obtained PE layer was back-extracted by a 40% ethanol alkaline solution with 0.2 M NaOH, and then it was used for SERS detection. The whole process can be completed in ten minutes. The relative flow chart is shown in Fig. 4 (the green/red line represents the optimal/control process).

For the first step, the effect of ethanol was to improve the solubility of the analyte in aqueous solvent. However, a low proportion of ethanol solution led to the reduction of extraction efficiency, and its high proportion resulted in excessive extraction of matrix molecules. According to the influence of ethanol (extraction solution) on the SERS signal (Fig. S7), 7.5% ethanol was selected as the optimal proportion. From the perspective of the matrix, the obtained supernatant mainly contained the matrix molecules with aqueous solubility advantage (included oil and non-oil soluble).

For the second step, the function of PE was used to extract the organic target molecules from aqueous phase, and exclude most of the non-oil soluble matrix molecules. However, in the aqueous phase, non-polar PE did not have sufficient distribution advantage for polar organophosphorus molecule. In order to improve the distribution ratio of MTDT in the organic phase versus the aqueous phase, NaCl solid was added to the aqueous phase in advance to increase the ion concentration and promote the organic molecules to be driven in the organic phase. The detection result (inset of Fig. 4) shows that the addition of NaCl contributed greatly to the signal enhancement, although this might have interfused some polar matrix molecules to the next step.

For the third step, ethanol has a similar purpose as in the first step, but at a relative high proportion. This is due to the amounts of matrix molecules in the organic phase has been drastically reduced in the above steps. Moreover, most of the remaining oil-soluble matrix molecules in PE phase were effectively repelled by aqueous phase. Instead of extracting MTDT directly from organic phase for further alkaline hydrolysis, NaOH was included in the aqueous phase in advance to obtain the MTMT. The interfacial exchange of the two insoluble phases enabled the alkaline hydrolysis reaction between the OH^- and MTDT (inset of Fig. 4). In addition, the NaOH solution did not need extra addition in the subsequent detection step. Because the MTMT has a better aqueous solubility than MTDT (attributed to the lack of phosphate ester groups and exposure of thiol groups), it can be extracted more efficiently by the aqueous phase. Hence, as shown in the inset of detection step in Fig. 4, it appeared an obvious signal advantage compared with the direct extraction of MTDT in the third step.

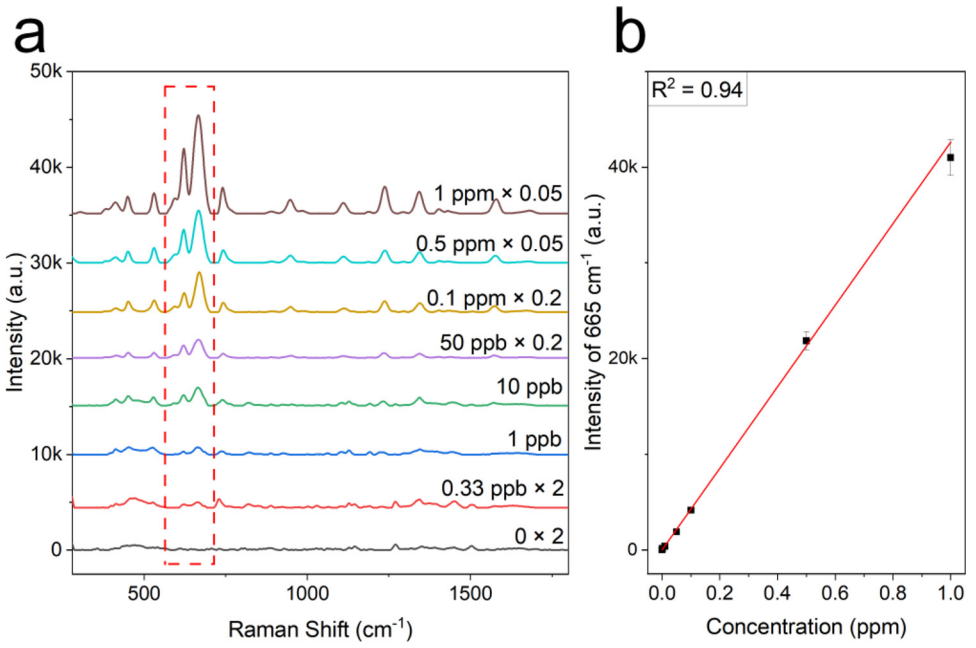


Figure 3. (a) SERS spectra after MTDT alkaline hydrolysis under different concentration gradients and (b) the linear relationship between spectra strength (655 cm^{-1}) and concentration (0-1 ppm).

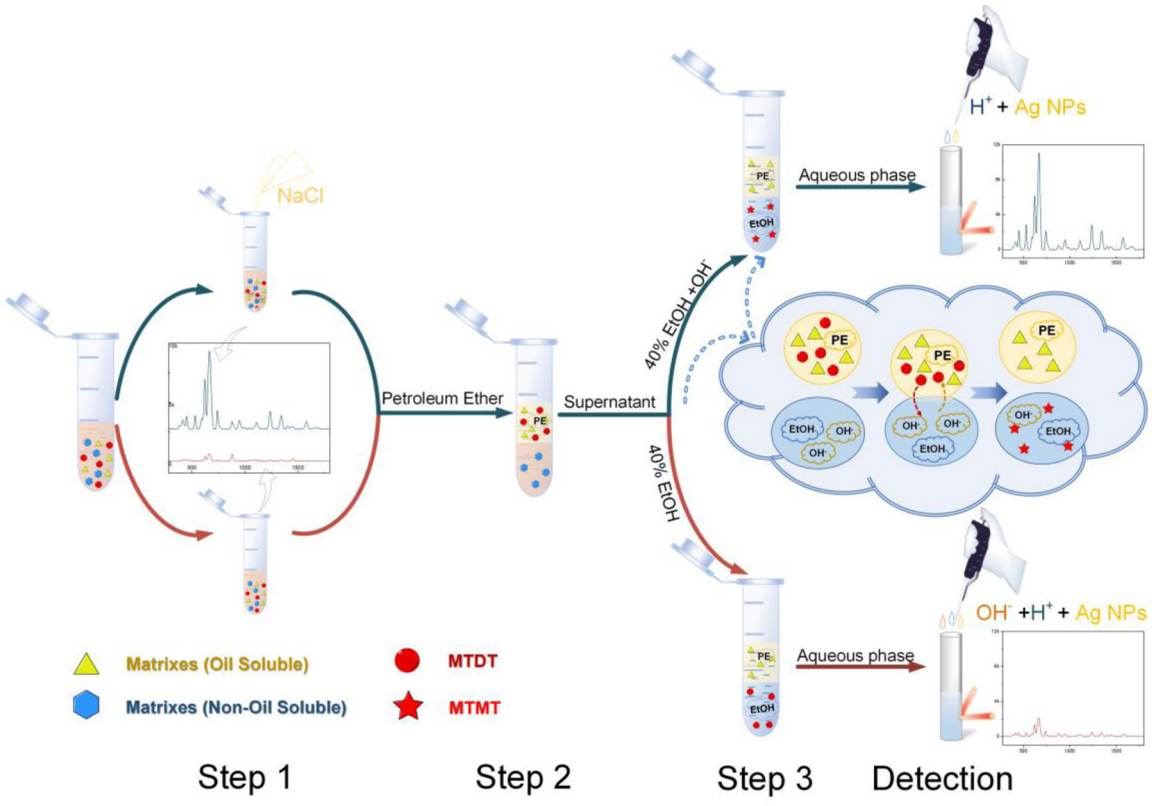


Figure 4. Flow chart of pre-treatment for the determination of MTDT in fruits, the green/red line represents the optimal/control process.

Compared with previously used other pre-treatment methods, including LLE and solid phase extraction (SPE) [8,11,14,16,47,48]. The above pre-treatment method possesses the advantages of rapid, simple operation, cost-effective and nontoxic. It is also important that, in the following section, a detection limit satisfying the MRL requirement can be reached in various fruits.

3.5. Detection limits in various fruit samples

Six kinds of fruit (orange, apple, pear, grape, tomato, pitaya) were used as real experiment objects (Fig. 5a), which contain different matrix components. Fig. S8 shows the experimental phenomenon of the pre-treatment steps for each sample. Fig. 5b–g show SERS signals in the

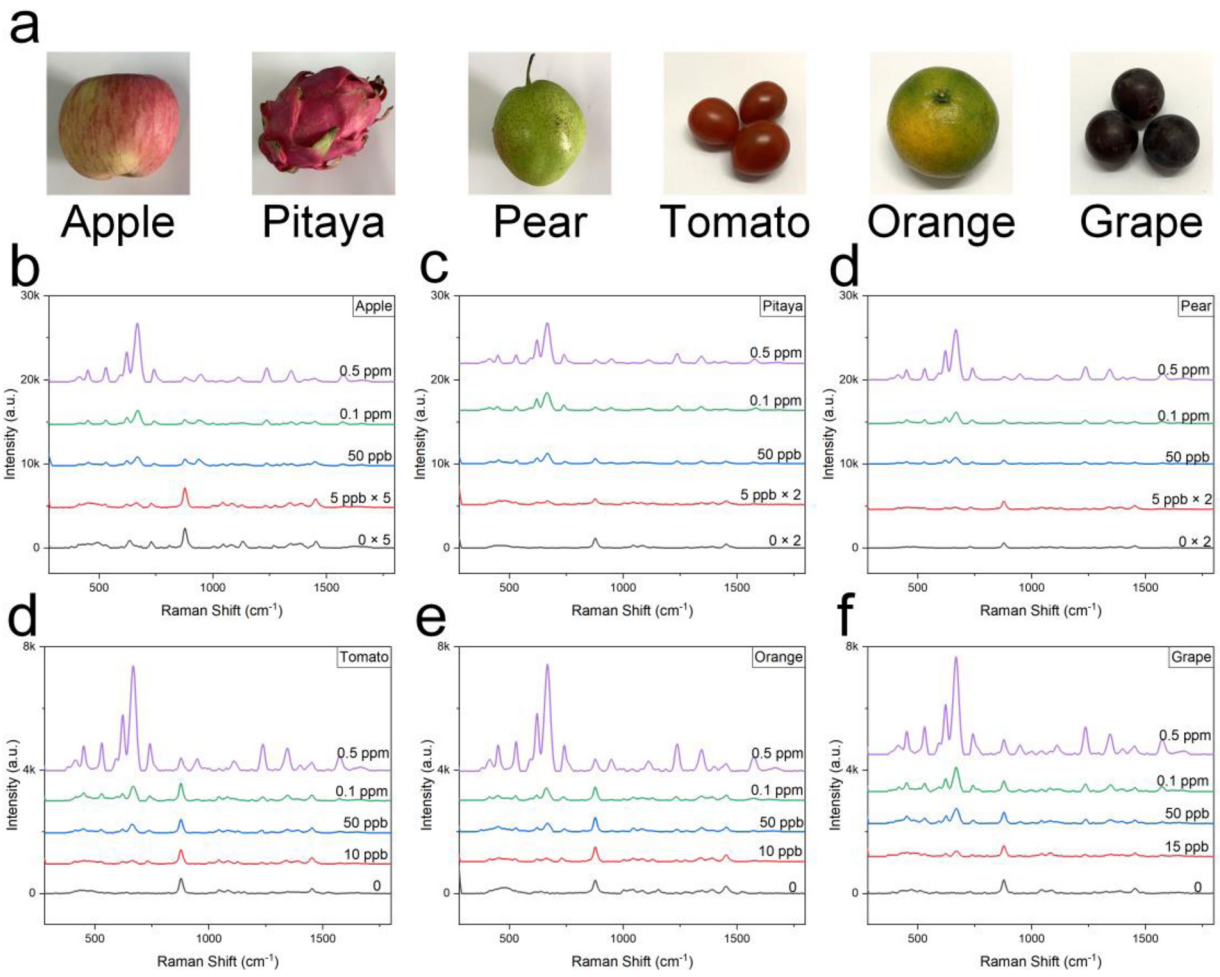


Figure 5. (a) Image of different fruits used in the experiments. (b–f) SERS signals in the different spiked fruit samples with gradient concentrations (0–0.5 ppm).

Table 2
The LODs of different fruits in this study and their MRLs required by China.

Friuts	LODs (ppb)	MRLs (ppb)(GB 2763-2021)
Apple	5	50
Pitaya	5	50
Pear	5	50
Orange	10	50
Tomato	10	50
Grape	15	50

spiked samples with gradient concentrations (0–0.5 ppm). The SERS peaks from the spectra of real samples were in good agreement with the standard sample, and no obvious interferential peak of matrix were found, indicating the effectiveness and reliability of the pre-treatment method. Similarly, the highest peak, 662 cm^{-1}, was used as the characteristic peak for qualitative identification, and the three times of SNR considered as the threshold of detection limit, i.e., 5–15 ppb were determined as the LODs in different fruits, as shown in Table 2. These values are much lower than the MRL required in China (50 ppb). Moreover, Table 3 summarizes the performance of previous researches on the detection of MTDT [8,9,11,13, 15, 17,18,25-27,49,50]. Compared with other SERS methods, the detection limit in this study was greatly improved and even superior to the detection level of some other mainstream technologies.

3.6. Quantitative analysis

Apple was selected as the object for quantitative analysis. A total of 251 SERS spectra distributed in different adding concentrations (0–5 ppm in homogeneous fruit samples) were collected and their baseline correction were performed (Fig. 6a). Six significant characteristic peaks (530, 622, 665, 740, 1235 and 1343 cm^{-1}) were used as the fitting objects for UVA/MVA. The intensity of these peaks (±3 cm^{-1}) was read automatically by a program written on MATLAB. To clearly identify each peak, 10 ppb was used as the minimum spiked concentration. Then, the univariate/multivariate linear regression (ULR/MLR) equations were established for the relationship between the concentration of MTDT in spiked samples and the intensity of characteristic peaks. As shown in Fig. S9, for the UVA, it is clear that the determination coefficient of different individual peak was ranged from 0.8661 to 0.9138 in the univariate linear fitting result. And then, four peaks (530, 665, 1235 and 1343 cm^{-1}) with high determination coefficients were selected as MVA variables. For the MVA, as shown in Table S1, the combinations of different peaks have great influence on the linear regression equation. Under the case of specified individual variable and variables combination (Fig. 6b), MLR equations have a higher determination coefficient than ULR equations and increased with the number of variates. This is due to the MLR equation uses the least square method to estimate the coefficient vector, and assigns different weight to each characteristic peak. Therefore, MLR can use more peaks information than ULR, and these peaks combination better explain the concentration information.

Table 3
Summarization of the performance of previous researches on the determination of MTDT.

References	Detection method	Pre-treatment method	Sensitivity **Std**	**Real samples**	Time consumption
This work	SERS with alkaline hydrolysis strategy	Self-developed LLE approach	0.33 ppb	Apple, pear, pitaya: 5 ppb. Orange, tomato: 10 ppb. Grape: 15 ppb	About 10 min
2019 *Talanta* [27]	SERS with silver-loaded chitosan foam substrate	–	μg level	–	About 30 min (water sample)
2019 *AIP Advances* [26]	SERS with silver solid substrate	–	0.1 ppm	–	In a few minutes (water sample)
2013 *Analytical Methods* [25]	SERS combined with thin layer chromatography	LLE approach	0.1 ppm	Tea samples: ppm level	More than 1 hour
2021 *Journal of Agriculture and Food Chemistry* [17]	Fluorescence with CdTe-QD sensors	–	0.027 ppb	–	More than 1 hour (water sample)
2021 *Analytical Chemistry* [18]	Fluorescence with AChE-catalyzed hydrolysis strategy	–	0.015 ppb	–	More than 1 hour (water sample)
2015 *Food Analytical Methods* [13]	HPLC	Modified QuEChERS method	–	Tomato: 33 ppb (LOD) & 110 ppb (LOQ)	Several hours
2015 *RSC Advances* [15]	UHPLC-MS	Carbon nanotube-based QuEChERS extraction	–	Dried tangerine: 0.4 ppb (LOD) & 1 ppb (LOQ)	Several hours
2015 *Journal of Chromatography A* [9]	GC–NPD	Magnetic nano-adsorbent SPE	0.1 ppb (LOD) & 0.3 ppb (LOQ)	Validated in spiked samples (5 ppb in apple, grape, pear, bell pepper and celery)	Several hours
2019 *Analytical Methods* [11]	GC-MS	self-developed LLE approach	–	Blank biobed extract: 1 ppb (LOD) & 50 ppb (LOQ)	Several hours
2016 *Journal of Agriculture and Food Chemistry* [8]	Sweeping micellar electrokinetic chromatography	Ultrasound-assisted dispersive liquid–liquid microextraction	–	Lycium chinense: 7 ppb, Dioscorea opposite: 8 ppb	Several hours
2017 *Electrochimica Acta* [49]	Electrochemical method with NA/Ag@rGO-NH2/AChE/GCE biosensor	–	9.5 ppb	–	About 1 hour (water sample)
2014 *Talanta* [50]	Electrochemical method with MIP/sol-gel impedimetric sensor	—	5.14 ppb	–	More than 20 min (water sample)

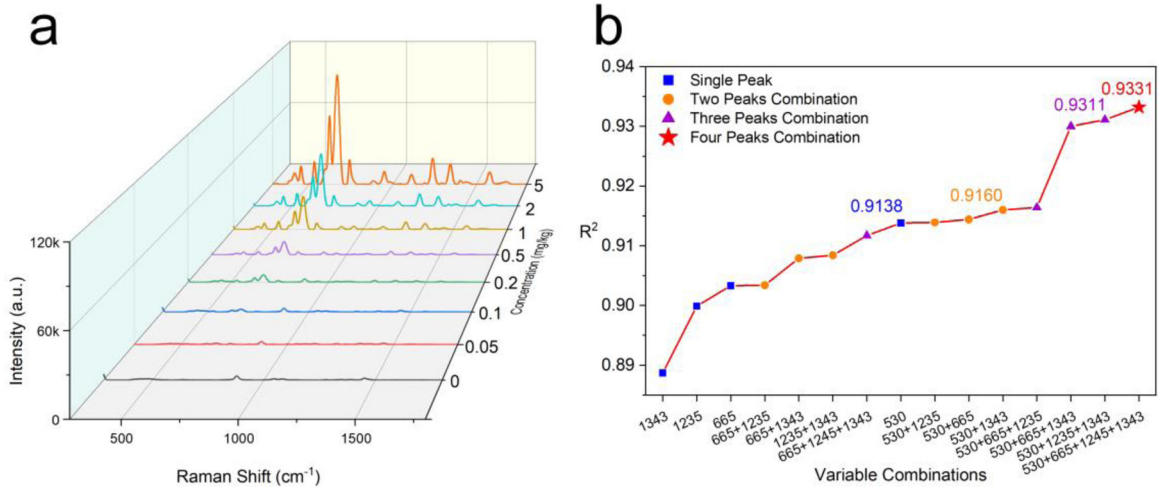


Figure 6. (a) Average SERS spectra of spiked apple samples with different concentrations of MTDT (0–5 ppm). (b) The determination coefficient of different individual peak and peaks combinations, obtained from UVA and MVA.

So that it can be applied to solve the problem of quantitative analysis caused by the complex change of peak intensity in practical application. Hence, the MLR equation with four variates was selected as the quantitative analysis equation. As follow:

$$Y = 2.8804 \times 10^{-4} \times x_1 + 4.4880 \times 10^{-5} \times x_2 + 3.4107 \times 10^{-4} \times x_3 - 7.3207 \times 10^{-4} \times x_4.$$

x_1, …, x_4 represent the different variables, and the corresponding determination coefficient is 0.9331.

Then, five groups of parallel experiments were performed to calculate the recovery rates with the MLR quantitative analysis equation. As shown in Table S2, the recovery rates, range from 98% to 112%, were obtained. Which indicated that the MVA method was suitable for the

quantitative analysis of MTDT in fruit based on our detection and pretreatment methods.

4. Conclusion

In this study, a novel and practical route for the detection of MTDT in various fruits has been developed, which based on the alkaline hydrolysis strategy and spherical Ag NPs SERS substrate.

DMTP and MTMT were generated via S_N2 substitution reaction under an alkaline condition, and the obtained sensitive and distinctive SERS signal was verified to be derived from MTMT which has a higher Raman response as compared to pure MDTD and DMTP. After adjusting the ion environment in the detection solution by hydrochloric acid, the LOD of MTDT was achieved up to 0.33 ppb in water. In the practical application system, an innovative and facile method was used for the pretreatment of various fruits to achieve the specific detection of MTDT in ten min, up to the detection limits of 5–15 ppb in different fruits. This is approximately one order of magnitude lower than the MRL required by China, US and the EU. Finally, the MVA method was used for the quantitative analysis and the optimal MLR equation was established from four characteristic variables. Compared with UVA, MVA obtained a better dynamic range (10 ppb to 5 ppm). Therefore, we believe that this work will impart new contributions and further ideas for the application of SERS method in practical complex system.

Declaration of interests

The authors declare that they have no known competing financial interests or personal relationships that could have appeared to influence the work reported in this paper.

Acknowledgements

This work was supported by the Natural Science Foundation of Zhejiang Province [LY21C200001], National Key R&D Program of China [2017YFD0401302], National Natural Science Foundation of China [62105245], Natural Science Foundation of Zhejiang [LQ20F030059], Wenzhou Science Technology Bureau General Project [S2020011].

Supplementary materials

Supplementary material associated with this article can be found, in the online version, at doi:10.1016/j.cjac.2022.100107.

Reference

[1] Walker GP, Richards CB, Jones WG, Aitken DCG. J Eco Entomol 1991;84(1):17–24. doi:10.1093/jee/84.1.17.
[2] Papastergiou SG, Koukoulias NE, Ziogas E, Dimitriadis T, Koumis P. BMJ Case Reports 2009;2009:12–18 nov24 1. doi:10.1136/bcr.09.2009.2256.
[3] Gungordu A. Aqua Toxicol 2013:220–8 140-141. doi:10.1016/j.aquatox.2013.06.012.
[4] Quest JA, Copley MP, Hamernik KL, Rinde E, Fisher B, Engler R, et al. Regul Toxicol Pharmacol 1990;12(2):117–26. doi:10.1016/S0273-2300(05)80053-4.
[5] Sánchez L, Romero E, Peña A. Chemosphere (Oxford) 2005;59(7):969–76. doi:10.1016/j.chemosphere.2004.09.108.
[6] Li C, Zhu H, Li C, Qian H, Yao W, Guo Y. Food Chem 2021;354:129552. doi:10.1016/j.foodchem.2021.129552.
[7] Cabras P, Angioni A, Garau VL, Melis M, Pirisi FM, Karim M, et al. J Agric Food Chem 1997;45(6):2244–7. doi:10.1021/jf960922e.
[8] Wei J-C, Hu J, Cao J-L, Wan J-B, He C-W, Hu Y-J, et al. J Agric Food Chem 2016;64(4):932–40. doi:10.1021/acs.jafc.5b05369.
[9] Mahpishanian S, Sereshti H, Baghdadi M. J Chromatogr a 2015;1406:48–58. doi:10.1016/j.chroma.2015.06.025.
[10] Albero B, Sánchez-Brunete C, Tadeo JL. J Agric Food Chem 2003;51(24):6915–21. doi:10.1021/jf030414m.
[11] Vareli CS, Pizzutti IR, Gebler L, Cardoso CD, Fontana MEZ, Reichert B, et al. Analytica Methods 2019;11(42):5455–63. doi:10.1039/c9ay01746a.
[12] Fang G, Min G, He J, Zhang C, Qian K, Wang S. J Agric Food Chem 2009;57(8):3040–5. doi:10.1021/jf803913q.
[13] Bedassa T, Gure A, Megersa N. Food Analytica Methods 2015;8(8):2020–7. doi:10.1007/s12161-014-0081-7.
[14] Bakas I, Ben Oujji N, Moczko E, Istamboulie G, Piletsky S, Piletska E, Ait-Ichou I, Ait-Addi E, Noguer T, Rouillon R. Analytica Chimica Acta 2012;734:99–105. doi:10.1016/j.aca.2012.05.013.
[15] Dou X, Chu X, Kong W, Yang Y, Yang M. RSC Advances 2015;5(105):86163–71. doi:10.1039/c5ra15348d.
[16] Kuang Y, Qiu F, Kong W, Luo J, Cheng H, Yang M. J Chromatogr B, Analytica Tech Biomed Life Sci 2013;939:98–107. doi:10.1016/j.jchromb.2013.09.013.
[17] Yang Q, Li Q, Li H, Li F. J Agric Food Chem 2021;69(9):2689–96. doi:10.1021/acs.jafc.0c08212.
[18] Li Q, Wu J, Yang Q, Li H, Li F. Analytica Chem (Washington) 2021;93(19):7362–8. doi:10.1021/acs.analchem.1c01414.
[19] Itoh T, Yamamoto YS. Nanoscale 2021;13(3):1566–80. doi:10.1039/d0nr07344j.
[20] Langer J, Jimenez de Aberasturi D, Aizpurua J, Alvarez-Puebla RA, Auguié B, Baumberg JJ, Bazan GC, Bell SEJ, Boisen A, Brolo AG, Choo J, Cialla-May D, Deckert V, Fabris L, Faulds K, García de Abajo FJ, Goodacre R, Graham D, Haes AJ, Haynes CL, Huck C, Itoh T, Käll M, Kneipp J, Kotov NA, Kuang H, Le Ru EC, Lee HK, Li J-F, Ling XY, Maier SA, Mayerhöfer T, Moskovits M, Murakoshi K, Nam J-M, Nie S, Ozaki Y, Pastoriza-Santos I, Perez-Juste J, Popp J, Pucci A, Reich S, Ren B, Schatz GC, Shegai T, Schlücker S, Tay L-L, Thomas KG, Tian Z-Q, Van Duyne RP, Vo-Dinh T, Wang Y, Willets KA, Xu C, Xu H, Xu Y, Yamamoto YS, Zhao B, Liz-Marzán LM. ACS Nano 2020;14(1):28–117. doi:10.1021/acsnano.9b04224.
[21] Chen S, Meng L, Wang L, Huang X, Ali S, Chen X, et al. Sens Actuators B Chem 2021;348:130706. doi:10.1016/j.snb.2021.130706.
[22] Luo X, Pan R, Cai M, Liu W, Chen C, Jiang G, et al. Sens Actuators B Chem 2021;326:128826. doi:10.1016/j.snb.2020.128826.
[23] Choi H-K, Park W-H, Park C-G, Shin H-H, Lee KS, Kim ZH. J Amer Chem Soc 2016;138(13):4673–84. doi:10.1021/jacs.6b01865.
[24] Xia C, Zhang D, Li H, Li S, Liu H, Ding L, Liu X, Lyu M, Li R, Yang J, Li Y. Nano Research 2022;15:694–700. doi:10.1007/s12274-021-3549-y.
[25] Yao C, Cheng F, Wang C, Wang Y, Guo X, Gong Z, et al. Analytica Methods 2013;5(20):5560–4. doi:10.1039/c3ay41152d.
[26] Lin G, Zhu J, Wu M, Lu P, Wu W. AIP Advances 2019;9(3):035203. doi:10.1063/1.5063969.
[27] Wang C, Wong KW, Wang Q, Zhou Y, Tang C, Fan M, Mei J, Lau W-M. Talanta (Oxford) 2019;191:241–7. doi:10.1016/j.talanta.2018.08.067.
[28] Becke AD. J Chem Phys 1993;98(7):5648–52. doi:10.1063/1.464913.
[29] Becke AD. J Chem Phys 1996;104(3):1040–6. doi:10.1063/1.470829.
[30] Jamroz MH. Spectrochimica Acta. Part A, Mol Biomol Spectrosc 2013;114:220–30. doi:10.1016/j.saa.2013.05.096.
[31] Chen Y, Liu H, Li X, Tang S, Gu C, Wei G, et al. Sens Actuators B: Chem 2021;339:129856. doi:10.1016/j.snb.2021.129856.
[32] Hassanien AS, Khatoon UT. Physica B: Condensed Matter 2019;554:21–30. doi:10.1016/j.physb.2018.11.004.
[33] Chen Y, Liu H, Tian Y, Du Y, Ma Y, Zeng S, et al. ACS Appl. Mater. Interfaces 2020;12(12):14386–99. doi:10.1021/acsami.9b22725.
[34] Tang S, Liu H, Tian Y, Chen D, Gu C, Wei G, et al. Spectrochimica Acta Part A: Mol Biomol Spectrosc 2021;262:120092. doi:10.1016/j.saa.2021.120092.
[35] Hebié S, Holade Y, Maximova K, Sentis M, Delaporte P, Kokoh KB, Napporn TW, Kabashin AV. ACS Catalysis 2015;5(11):6489–96. doi:10.1021/acscatal.5b01478.
[36] Chen X, Huang X, Chen S, Ali S, Chen X, Yuan L, et al. Sens Actuators B: Chem 2022;359:131584. doi:10.1016/j.snb.2022.131584.
[37] Ma Y, Du Y, Chen Y, Gu C, Jiang T, Wei G, et al. Chem Eng J 2020;381:122710. doi:10.1016/j.cej.2019.122710.
[38] Cai WB, Ren B, Li XQ, She CX, Liu FM, Cai XW, et al. Surf Sci 1998;406(1):9–22. doi:10.1016/S0039-6028(97)01030-3.
[39] Le Ru EC, Blackie E, Meyer M, Etchegoin PG. J Physica Chem. C 2007;111(37):13794–803. doi:10.1021/jp0687908.
[40] Mikołajczyk M, Ziemnicka B, Krzywański J, Cypryk M, Gostyński B. Mol 2021;26(12):3655 Basel, Switzerland. doi:10.3390/molecules26123655.
[41] Cox Jr JR, Ramsay OB. Chem Rev 1964;64(4):317–52. doi:10.1021/cr60230a001.
[42] Dyguda-Kazimierowicz E, Sokalski WA, Leszczynski J. J Physica Chem. B 2008;112(32):9982–91. doi:10.1021/jp800386f.
[43] López-Canut V, Roca M, Bertrán J, Moliner V, Tuñón I. J Amer Chem Soc 2010;132(20):6955–63. doi:10.1021/ja908391v.
[44] Wu D-Y, Li J-F, Ren B, Tian Z-Q. Chem Soc Rev 2008;37(5):1025–41. doi:10.1039/b707872m.
[45] Zhao LJensen, Schatz GC. J Amer Chem Soc 2006;128(9):2911–19. doi:10.1021/ja0556326.
[46] Otto A, Billmann J, Eickmans J, Ertürk U, Pettenkofer C. Surf Sci 1984;138(2–3):319–38. doi:10.1016/0039-6028(84)90251-6.
[47] Wan Ibrahim WA, Veloo KV, Sanagi MM. J Chromatogr A 2012;1229:55–62. doi:10.1016/j.chroma.2012.01.022.
[48] Liu W, Hu Y, Zhao J, Xu Y, Guan Y. J Chromatogr A 2006;1102(1):37–43. doi:10.1016/j.chroma.2005.10.026.
[49] Guler M, Turkoglu V, Basi Z. Electrochimica Acta 2017;240:129. doi:10.1016/j.electacta.2017.04.069.
[50] Bakas I, Hayat A, Piletsky S, Piletska E, Chehimi MM, Noguer T, Rouillon R. Talanta (Oxford) 2014;130:294–8. doi:10.1016/j.talanta.2014.07.012.